

VII. ELECTRODYNAMICS OF MEDIA *

Academic and Research Staff

Prof. L. J. Chu
Prof. H. A. Haus

Prof. P. W. Hoff
Prof. J. A. Kong
Prof. P. Penfield, Jr.

Dr. L. Frenkel
T. E. Sullivan

Graduate Students

H. Granek
E. R. Kellet, Jr.

D. L. Lyon

E. E. Stark, Jr.
L-h. Wang

A. AN EXPERIMENTAL DETERMINATION OF CROSS RELAXATION IN CO₂

The purpose of the experiments reported here is to study the relative strength of the various relaxation processes in a CO₂ laser at 10.6 μm ; the relaxation of the population in velocity groups within a single line, and the relaxation of the population in different rotational levels. The experiments represent a refinement of experiments reported previously.¹ Sufficient data have been obtained to determine the relaxation rates of interest.

A saturating CO₂ laser tuned to the P(20) transition at 10.6 μm is chopped at 260 Hz and modulates the population in a CO₂ cell (Fig. VII-1). A low-intensity beam, colinear with the saturating beam and with its polarization at right angles to that of the saturating beam and isolated through a polarizer is used to probe the effect of the modulation on the gain or absorption in the cell. The probe beam is piezoelectrically tunable across the linewidth of six R transitions. The sweep of the piezoelectric oscillator can be calibrated in frequency by beating this laser against the fixed laser on the same line. The probe beam is separated beyond the amplifier by a grating and after detection is synchronously amplified at the chopper frequency. The saturating oscillator also contains a piezoelectric tuner and its frequency can be adjusted within the P(20) transition.

A theory of cross relaxation describing the phenomena in the CO₂ laser has been presented previously. The theory included three rate parameters: the rate of relaxation within the velocity profile of a single energy level, $1/\tau$, the rate of cross relaxation among rotational levels,² Λ , and the rate of relaxation out of the vibrational energy states, γ . In the previous analysis, it was assumed that negligible velocity changes occur as the particles change rotational levels. The consequence of this assumption is that a saturating laser would produce a population

*This work was supported by the Joint Services Electronics Programs (U.S. Army, U.S. Navy, and U.S. Air Force) under Contract DA 28-043-AMC-02536(E), and in part by U.S. Air Force (ESD) Contract F19628-70-C-0064.

(VII. ELECTRODYNAMICS OF MEDIA)

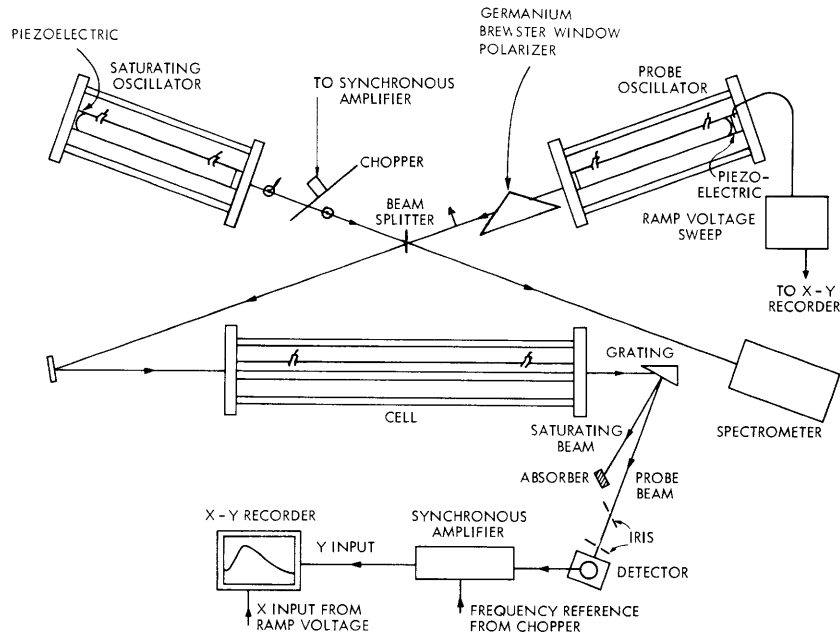


Fig. VII-1. Experimental arrangement.

decrease in all upper rotational levels over the homogeneous linewidth, in addition to an over-all pull-down of each of the levels. A corresponding fine structure would appear in all lower levels. The experiments are matched better by a theory that assumes that the particles may change velocity appreciably when they change rotational level. The rate equation describing this process is given below for the upper rotational levels.

$$\begin{aligned} \dot{n}_j(v) = & -\gamma n_j(v) - \int \Gamma(v', v) n_j(v) dv' + \int \Gamma(v, v') n_j(v') dv' - \sum_k \int \Gamma_{kj}(v', v) n_j(v) dv' \\ & + \sum_k \int \Gamma_{jk}(v, v') n_k(v) dv' - W(v) \left[n_\ell(v) - \frac{g_{\text{upper}}}{g_{\text{lower}}} n_{\ell'}(v) \right] \delta_{j\ell} + R_j(v). \end{aligned}$$

Here the notation coincides with that reported previously. Only in the induced transition rate is the lower level explicitly indicated. The subscript ℓ applies to the lasing level. The assumption of complete randomization after one collision is made. That is,

$$\Gamma(v', v) n_j^e(v) = \Gamma(v, v') n_j^e(v') = \frac{1}{\tau} \frac{n_j^e(v) n_j^e(v')}{\int n_j(v) dv}$$

$$\Gamma_{KJ}(v', v) n_J^e(v) = \Gamma_{JK}(v, v') n_K^e(v') = \Lambda \frac{n_J^e(v) n_K^e(v')}{\sum_m N_m^e}.$$

A corresponding rate equation can be set up for the lower level. In general, different relaxation rates would have to be assumed for the lower level. It is to be expected, however, that the rotational cross-relaxation rates should depend only weakly on the vibrational state of the system. Hence, one might expect the Λ 's for the upper and lower levels to be the same. The same can be expected about the velocity cross-relaxation rate, $1/\tau$. Clearly, the vibrational cross-relaxation rate γ cannot be assumed, in general, to be independent of the vibrational state. In our experiment we have found, however, that the rate at which particles leave the interaction with the saturating beam or probe beam is not determined by the internal vibrational relaxation rate, but rather is dominated by spatial diffusion in view of the low pressure (1 Torr or less) employed in the experiment. This fact has two consequences. First, it means that the vibrational relaxation rate cannot be determined from our experiment. Second, however, it implies a great simplification because in this way all of the relaxation rates of the upper level become equal to the corresponding relaxation rates of the lower level. Solving the rate equations for the upper level and the corresponding rate equations for the lower level, we find the following expressions for the signal detected in the experiment:

$$\frac{\Delta a(v)}{R(18)} = -\delta p N_{19}^e f(v) \left[\overline{W} \left(sd + \frac{39}{37} \frac{N_{18}^e}{N_{20}^e} \frac{sd+1}{1 + \frac{\gamma}{\Lambda/z}} + W(v) \right) \right] \quad (3)$$

$$\frac{\Delta a(v)}{R(20)} = -\delta p f(v) \left[\overline{W} \left(\frac{sd+1}{1 + \frac{\gamma}{\Lambda/z}} N_{21} + \frac{43}{41} N_{19}^e sd \right) + \frac{43}{41} N_{19} W(v) \right] \quad (4)$$

$$\frac{\Delta a(v)}{R(J)} = -\delta p f(v) \left(\frac{sd+1}{1 + \frac{\gamma}{\Lambda/z}} \right) \left[\overline{W} \left(N_{J+1}^e + N_J^e \frac{2J+3}{2J+1} \frac{N_{19}^e}{N_{20}^e} \right) \right], \quad J \neq 18, 20 \quad (5)$$

where

$$\delta \equiv 1 - \frac{39}{41} \frac{N_{20}^e}{N_{19}^e}, \quad p \equiv \frac{\lambda^2}{8\pi t_{sp} \left[\gamma + \frac{1}{\tau} + \Lambda \left(1 - \frac{1}{z} \right) \right]}$$

(VII. ELECTRODYNAMICS OF MEDIA)

$$s \equiv \frac{(\gamma + \Lambda/z)}{\gamma(\gamma + \Lambda)}, \quad d \equiv \frac{1}{\tau} + \frac{\Lambda(1 - 1/z)}{1 + \frac{\gamma}{\Lambda/z}}$$

$$z \equiv \frac{\sum_m N_m^e}{N_\ell}$$

and λ and t_{sp} are, respectively, the wavelength and spontaneous lifetime. Equation 3 holds for the case when the probing signal shares a common upper level with the saturating signal; Eq. 4 when the probing signal shares a common lower level; and Eq. 5 when the probe and the saturating oscillator have no common levels. From the observation of the signal vs frequency of the probe laser, one may determine the relaxation rates γ , $1/\tau$, and Λ . One further note of caution is in order. The theory contains only three relaxation rates, whereas the actual situation calls for several more: the rate of relaxation among the different vibrational excitations in the same vibrational mode; the rate of relaxation between CO_2 and N_2 levels when N_2 is added. The actual experiment only measures three parameters. A more detailed theory, with more than three relaxation rates arrives at final equations for the three parameters measured which contain combinations of all relaxation rates. Because of the relative magnitudes of $\frac{1}{\tau}$, Λ and γ , and of the other relaxation rates not included in the simple theory, one finds that the parameters s , p , and d of the simple theory are not greatly modified by the inclusion of the other relaxation rates. It was decided, therefore, to interpret the experiment in terms of the simple theory taking into account only three relaxation rates. Figure VII-2 shows the experimental result obtained when the saturating oscillator was operating at P(20) and a probe oscillator was operating at R(18). The pressures are as indicated. Note the very clear appearance of a "pip" which is due to the change of population induced by the saturating laser over the homogeneous linewidth of the material. Clear signals were obtained for the CO_2 - N_2 cell unexcited, as well as excited by a discharge. Also indicated in Fig. VII-2 is the signal obtained when only CO_2 was introduced into the cell. If all relaxation rates were dominated by collisional changes of energy and velocity, then one would expect that the addition of nitrogen to the CO_2 would decrease the signal level because the relaxation rates are increased. We found the opposite to be true. We explain this phenomenon by the fact that the relaxation rate γ was diffusion-dominated,³ and in fact decreased when the nitrogen was added to the cell. Computations of the magnitude of the diffusion effect confirmed this explanation. Figure VII-3 shows a curve obtained when the probe oscillator did not share a common level with the saturating oscillator.

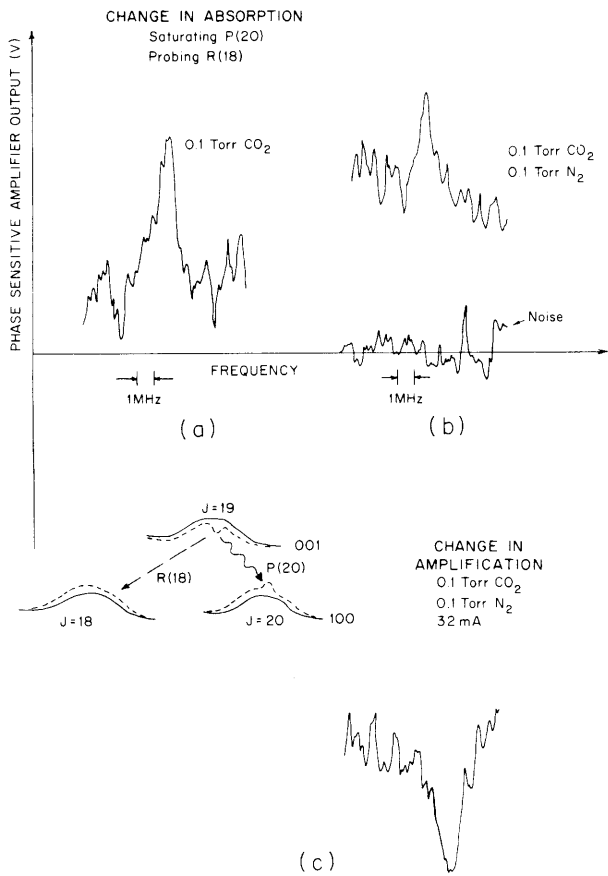


Fig. VII-2.
Signal as a function of frequency: saturating laser P(20); probe laser R(18).
(a) Unexcited, pure CO₂.
(b) Unexcited, CO₂-N₂ mixture.
(c) Discharge-excited, CO₂-N₂ mixture.

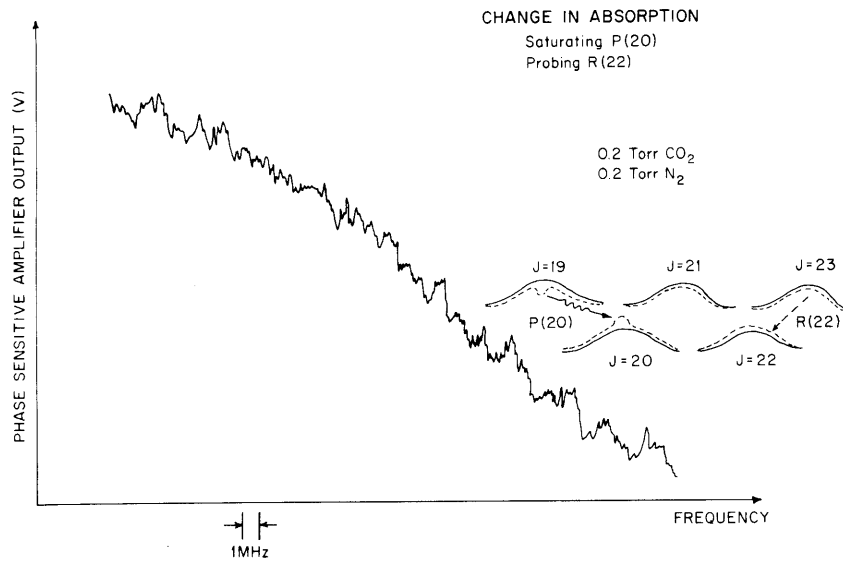


Fig. VII-3. Signal as a function of frequency; saturating laser P(20); probe laser R(16).

(VII. ELECTRODYNAMICS OF MEDIA)

Table VII-1. Summary of relaxation rates.

	Cold CO ₂	Cold CO ₂ - N ₂	Discharged CO ₂ - N ₂
γ [Torr/sec]	3.7×10^2	5.5×10^2	8.5×10^2
Δ [sec Torr] ⁻¹	5×10^6	9.9×10^6	11×10^6
$1/\tau$ [sec Torr] ⁻¹	12×10^6	13×10^6	12×10^6

The relaxation rates were determined from a total of 50 such experimental curves and are summarized in Table VII-1 in terms of relaxation rate as a function of pressure. A resonant absorption effect predicted by Hänsch and Toschek⁴ for co-traveling and countertraveling waves is not believed to be observable, because of the high M-degeneracy and orthogonal polarization. An analysis is in progress.

H. Granek, H. A. Haus

References

1. H. Granek, "An Experimental Determination of Cross Relaxation in CO₂," Quarterly Progress Report No. 96, Research Laboratory of Electronics, M.I.T., January 15, 1970, pp. 69-73.
2. P. K. Cheo and R. L. Abrams, "Rotational Relaxation Rate of CO₂ Laser Levels," Appl. Phys. Letters 14, 47 (1969).
3. C. P. Christensen, Jr., H. A. Haus, and C. Freed, "Effect of Diffusion on Gain Saturation in CO₂ Lasers," Technical Report 464, Lincoln Laboratory, M.I.T., Lexington, Massachusetts, February 7, 1969.
4. T. H. Hänsch and P. Toschek, "Perturbation Spectroscopy of Allowed and Forbidden Lines in a 3-Level Gas Laser," presented at The Sixth International Quantum Electronics Conference, Kyoto, Japan, September 7-10, 1970.

B. INVESTIGATION OF NONLINEAR EFFECTS IN
HIGH-PRESSURE CO₂ LASERS

We have been building and investigating high-pressure CO₂ laser systems,¹ with special emphasis on nonlinear interactions, mode locking, saturation broadening, and so forth. We have constructed two discharge tubes with the following characteristics²:

Tube 1: 2" OD × 3/16" wall × 4' Plexiglas.

Anode: 36" brass rod; 3/8" diameter.

Cathode: 191 - 1 KΩ (1/2 W) resistors, spaced 3/16" apart for a distance of approximately 35".

NaCl Brewster angle windows mounted at either end.

(VII. ELECTRODYNAMICS OF MEDIA)

Tube 2: 2" OD \times 3/16" wall \times 14" Plexiglas.

Anode: 12" brass rod; 3/8" diameter.

Cathode: 55 - 1 K Ω (1/2 W) resistors spaced 3/16" apart for a distance of approximately 11".

NaCl Brewster angle windows.

During normal operation a mixture of CO₂, N₂, and He gases in ratios of 1.5:1:11 are flowed through these tubes at rates of the order of 1/2 liter/min. Total pressure in the tubes is usually kept in the 250-350 Torr range. Voltages applied to the anode are in the 15-20 kV range. The lasers are pulsed by using a capacitor bank-spark gap circuit similar to the one described previously.² Capacitance for the long tube is 0.025 μ F, and for the short one 0.01 μ F. The discharge current pulses have a half-intensity width of \sim 1 μ s and peak amplitudes of 400 A and 250 A for the long and short tubes, respectively. Pulsing rates are in the 5-10 pps range.

Three experiments have been performed.

1. Observation of self-mode locking. Using the long tube in a 2.2 m optical cavity formed by a 4 m radius of curvature (50% transmissivity) Ge mirror and PTR grating the following observations were made with a Ge:Cu(Sb) liquid He-cooled detector. The laser output pulse lagged the discharge current pulse by \sim 2-3 μ s. The laser pulse envelope was filled with a very fast modulation (Fig. VII-4). The modulation had a depth of 100% and was nearly sinusoidal, with a frequency equal to the $c/2L$ intermode frequency spacing of the cavity (Fig. VII-5). The cavity length was shortened to 1.5 m and similar modulation behavior was observed.

The short tube was then used in a cavity, 0.5 m long, formed by an 80% reflectivity flat IRTRAN mirror and a high-reflectivity ($R=1.25$ m) aluminized mirror. The fast modulation was again observed, this time with frequency equal to 300 MHz ($=c/2L$), but the depth of modulation was not 100%. This could very likely be due to frequency response limitations in the Ge:Cu(Sb) detector³ or to the monitoring Tektronix 7704 oscilloscope.

From the shape of the modulation, we surmise that two modes, with possibly an admixture of one or two additional modes, are running stably in the laser. The detector is roughly an \mathcal{E}^2 sensitive device and from the figures we see that it was producing a steady-beat signal as an output. This steady beat may be viewed as a type of self-locking of the oscillating modes of the laser. It should be noted that the presence of self-locking was critically dependent on adjustment of the internal cavity aperture to the smallest settings allowable. Presumably this forces the laser to emit in the TEM₀₀ transverse mode.

The PTR grating was adjusted in the 2.2 m cavity so that the laser could be run in any one of 11 different P transitions at 10.6 μ (centered about P(20)). Self-mode locking

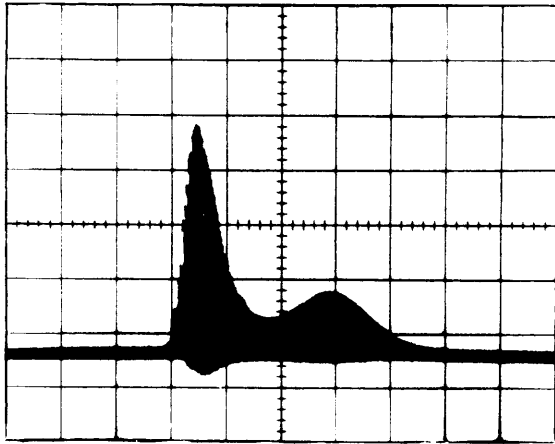


Fig. VII-4.

Giant laser pulse filled with self-locked modulation. Long tube: $L = 2.2$ m; 500 ns/div.

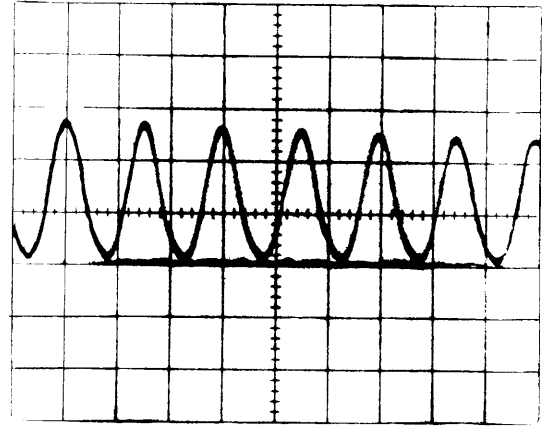


Fig. VII-5.

Same laser configuration as Fig. VII-4; self-locked pulses; 10 ns/div.

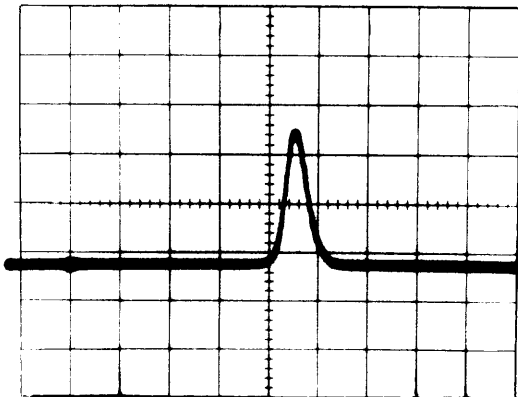


Fig. VII-6.

Giant laser pulse after 0.5 Torr SF_6 was added to intracavity cell. $L = 2.2$ m; 500 ns/div.

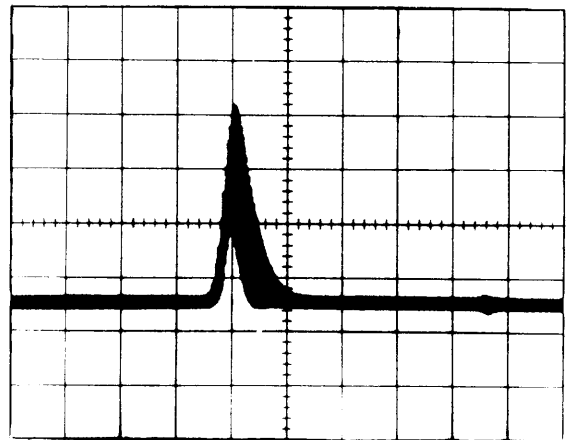


Fig. VII-7.

Giant laser pulse. 0.5 Torr SF_6 . PTR grating has been tuned to achieve locking. Same conditions as in Fig. VII-6. 500 ns/div.

was observed on all transitions. The self-locking was also observed at the 9.4μ transition of CO_2 .

2. Absorption by SF_6 . A cell with optical length of ~ 1 " was placed in both the long and short tube laser cavities near the flat mirror. The cell was positioned so that the optical beam was incident upon its NaCl end windows at the Brewster angle. With the laser running self-mode locked, the introduction of ~ 0.5 Torr of SF_6 generally killed the pulsing and left only a clean giant pulse envelope (Fig. VII-6). Presumably, the very strong frequency dependence of the SF_6 absorption⁴ has discriminated against one of the two oscillating modes and left us with only one mode above threshold. Slight tuning of the grating or the cavity length will bring back the mode-locked behavior (Fig. VII-7).

When He is added as a buffer gas to the 1" cell, the frequency dependence of the absorption is broadened. The characteristic relaxation time of the absorbing medium is thus shortened, and it seems possible that the SF_6 -He combination may act as a saturable absorber, producing even more strongly mode-locked pulses with a duty rate equal to $c/2L$, and pulse widths greatly narrowed. There has been some fast oscillation at approximately a 15 MHz rate in a 2.2 m cavity that has been induced by the cell. We believe this to be an optical ringing of the SF_6 -He gases at a frequency closely related to their T_1 relaxation times. Further study is being made of this system.

3. Amplification. The short tube was placed in a 1 m cavity formed by a flat 80% reflectivity mirror and an $R = 1.25$ m high reflectivity mirror. The long tube was placed coaxially with the 1 m laser cavity so that the output would travel the entire length and thus be amplified by the inverted medium. Apertures were placed internal to the laser cavity and between the laser and the long amplifier tube. Preliminary observations showed that the power gain for the long tube is ~ 4 -5 dB. Varying the delay time between the discharge pulses in the two tubes had no startling effects. As long as the amplifier was fired within a time less than 1.5-2.0 μsec after the laser firing time, the amplification was roughly uniform for the entire giant pulse. For delays greater than $\sim 2 \mu\text{sec}$ between laser and amplifier firing times (in that order) only the latter portions of the giant pulse were amplified. It should be noted that no independent test was made to determine whether the amplifier was saturated at any time during the passage of the laser pulse.

Further amplification work is planned using high-pressure CO_2 lasers in conjunction with low-pressure cw CO_2 amplifiers. Also, the discharge tube design will be varied in order to study and maximize the gain of the medium and the output power of high-pressure lasers. One of our aims is to achieve saturation broadening of our mode-locked pulses through fast saturation of the amplifier medium.⁵

D. L. Lyon, E. V. George, H. A. Haus

(VII. ELECTRODYNAMICS OF MEDIA)

References

1. A. J. Beaulieu, Appl. Letters 16, 504 (1970).
2. E. V. George and L. D. Pleasance, Quarterly Progress Report No. 98, Research Laboratory of Electronics, M.I.T., July 15, 1970, p. 47.
3. T. J. Bridges, H. A. Haus, and P. W. Hoff, IEEE J. Quantum Electronics, Vol. QE-4, p. 777, 1968.
4. E. D. Hinkley, Appl. Phys. Letters 16, 351 (1970).
5. P. W. Hoff, H. A. Haus, and T. J. Bridges, Phys. Rev. Letters 25, 82 (1970).